

# Masseter muscle volume measured using ultrasonography and its relationship with facial morphology

Philip C. M. Benington\*, John E. Gardener\*\* and Nigel P. Hunt\*\*\*

\*Department of Orthodontics, Glasgow Dental Hospital and School, \*\*Department of Medical Physics, University College, London and \*\*\*Department of Orthodontics, Eastman Dental Institute for Oral Health Care Sciences, University of London, UK

**SUMMARY** The aims of this study were to measure the volume, cross-sectional area, thickness, width, and length of contracted masseter muscles in a sample of adults, four males and six females, using three-dimensional (3D) ultrasonography, and to correlate these measurements with the variations in facial morphology of the sample. The scans were carried out bilaterally using a hand-held probe carrying a magnetic positional sensor, which enabled a computer to reconstruct the images into a 3D array of slices. Measurements were made by the computer from the reconstructed images using specially written software. Cephalometric analysis initially involved seven angular, eight linear, and two proportional variables, but as these were strongly inter-dependent, the variables were reduced to four principal components prior to statistical comparison with the mean muscle variables.

The values found for muscle volume, cross-sectional area, and thickness were broadly consistent with those of previous investigators. Volume showed a significant, negative correlation with mandibular inclination including gonial angle ( $P \leq 0.001$ ), and a significant, positive correlation with total posterior face height and ramus height ( $P \leq 0.001$ ), and lower posterior face height percentage ( $P \leq 0.01$ ). Weaker correlations were found for length and thickness.

While the results support existing evidence that large masticatory muscles are associated with brachycephalism and *vice versa*, a cautious interpretation is necessary in view of the small sample size. The 3D ultrasonography system is at an experimental stage and requires further development and evaluation.

## Introduction

Certain parameters of masticatory muscle function have been shown to correlate with facial morphology, including electromyographic activity (Ahlgren, 1966; Ingervall and Thilander, 1974; Lowe and Takada, 1984; Ueda *et al.*, 1998) and occlusal force (Sassouni, 1969; Ringqvist, 1973; Ingervall and Helkimo, 1978; Proffit *et al.*, 1983). These investigators have found that stronger, more active muscles are associated with a tendency to parallelism of the jaws and other features of the short face syndrome (Opdebeeck and Bell, 1978).

With the advent of modern imaging techniques, it has become possible to measure the size of the masticatory muscles *in vivo*. Weijs and Hillen (1984a, 1986) correlated the cross-sectional area of the masticatory muscles in males with skull shape, using computer tomography (CT), having previously demonstrated that muscle cross-sectional areas were proportional to their corresponding physiological cross-sections (Weijs and Hillen, 1984b). Large masseter and medial pterygoid muscle areas were associated with subjects possessing small gonial angles and long

mandibles. Gionhaku and Lowe (1989) calculated masseter and medial pterygoid muscle volumes, and cross-sectional areas from CT scans of adult males with obstructive sleep apnoea. Masseter muscle volume showed a negative correlation with the steepness of the mandibular plane and the size of the gonial angle, and a positive correlation with posterior face height, ramus height, and the ratio of ramus height to anterior face height. Eckhardt and Harzer (1993) used CT to measure the volume of masseter, medial and lateral pterygoids, genioglossus, and tongue muscles. They concluded that an increasing volume of masseter muscle in subjects ranging from 12 to 39 years of age was related to an anterior growth direction of the mandible.

Magnetic resonance imaging (MRI) was used by Hannam and Wood (1989) who found a correlation between the cross-sectional area of masseter and bi-zygomatic width in 22 adults males. Van Spronsen *et al.* (1991), also using MRI, found positive, significant correlations between a linear combination of several transverse skull dimensions, and the maximal cross-sectional areas of the temporalis and masseter muscles.

Ultrasonography (US) has been used by a number of investigators to measure masseter muscle. Raadsheer *et al.* (1994) compared both US and MRI in the measurement of mid-belly masseter muscle thickness and showed US to be an accurate and reproducible imaging technique. Kiliaridis and Kalebo (1991) correlated masseter muscle thickness with certain transverse facial measurements taken from standardized photographs. Bakke *et al.* (1992) found a negative correlation between maximal thickness of the superficial portion of the human masseter muscle and anterior face height, vertical jaw relationship, and mandibular inclination. Ruf *et al.* (1994) found that masseter thickness and width correlated only weakly with small facial width and jaw divergence measurements taken from photographs of females. Kubota *et al.* (1998) found mean masseter muscle thickness to be positively correlated with mandibular ramus height, and the thickness of the alveolar process and mandibular symphysis, and negatively correlated with mandibular inclination.

Although linear and area measurements of isolated masticatory muscle cross-sections have already been shown to correlate with facial variables, the sites at which they have been taken have varied between investigators, making direct comparisons difficult. The volume of a muscle is a more comprehensive representation of its overall dimensions, taking into account its cross-section as well as its length. Masseter muscle length might be expected to correlate with facial form, since mandibular ramus height has been shown to vary with the vertical dimension of the face, being increased in short-faced subjects (Schendel *et al.*, 1976; Opdebeeck and Bell, 1978).

No study has been published to date in which muscle volume has been measured using US, although it is a non-invasive imaging technique, and has the advantages over CT and MRI of being relatively inexpensive and less complicated to use. This is partly because US has lagged behind these other techniques in establishing practical 3D visualization due to problems associated with acquiring and displaying 3D sets of data. One such problem is the background texture contained in US images, which is referred to as 'speckle', and is produced by a variety of effects, including acoustic interference. In addition, US generates non-zero signals only on local gradients of the acoustic properties, so that the essential character of the image is discontinuous. These problems and some of their possible solutions have been outlined by Gardener (1991).

A number of diagnostic applications of 3D US have been described in the literature. Hell *et al.* (1993) reported on a 3D US diagnostic tool for maxillofacial surgery, and subsequently produced images of the vascular structures of the neck using a probe guidance device to produce equidistant and parallel 2D US images (Hell, 1995). This system is apparently capable of volume measurements. The masseter is a superficially placed, quadrilateral muscle and, therefore, well suited to US scanning. The aims of this study were to measure masseter muscle volume on a small sample of subjects using a quantitative 3D US system developed by Gardener (1991) and to investigate its relationship with facial morphology.

## Subjects and methods

The sample consisted of four males and six females, all of whom were patients attending the orthognathic surgery planning clinic at the Eastman Dental Hospital, London. They were all post-adolescent with intact dentitions, no marked jaw asymmetries, and no history of orthodontic treatment or orthognathic surgery. The age range for the females was 15 years 7 months to 31 years 8 months, and for the males 20 years 11 months to 26 years 7 months. The subjects were selected to include a range of skeletal jaw discrepancies, both in the antero-posterior and vertical dimensions. Selection was based on examination of the subjects' lateral skull cephalograms, taken with the teeth in occlusion.

## Ultrasonography

All scans were carried out in the Ultrasonography Department of the Middlesex Hospital, London by one of the authors (JEG), using a real-time scanner (Acuson 128™, Acuson Corporation, Mountain View, CA) with a 38-mm wide, 7 MHz linear probe. The subjects were placed in a supine position, with their heads turned sideways to provide good access for the probe. A 2-mm thick stand-off (Geliperm Wet™, Geistlich-Pharma, Wolhusen, Switzerland) was placed directly over the masseter region, with US gel applied to both surfaces. The subjects were instructed to keep their heads still and clench their back teeth together during scan registration.

The angle of the probe during scanning was adjusted to produce the strongest echo from the mandibular ramus, achieved when the scan plane was perpendicular to its surface (Kiliaridis and Kalebo, 1991). In order to register the scan planes at right angles to the long axis of the muscle, the probe was visually orientated at an estimated 30 degrees to the Frankfort plane. This was consistent with the technique of Weijs and Hillen (1984b) and van Spronsen *et al.* (1991). The orientation of the probe was maintained manually, while the full length of the muscle was scanned from origin to insertion. Although early scans relied on a single sweep of the probe to

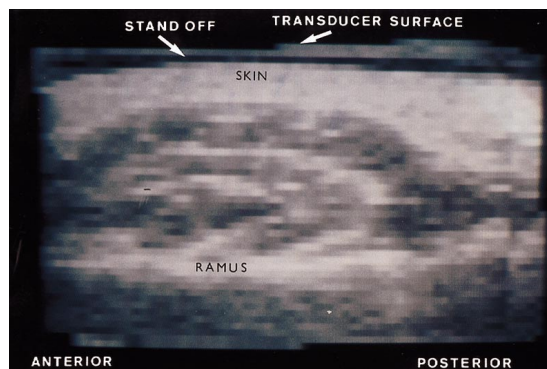


**Figure 1** Ultrasound image of masseter registered using a single scan sweep. A small section of the muscle has not been imaged due to the probe being of inadequate width.

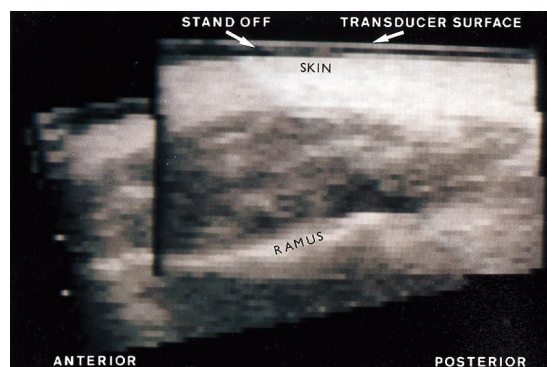


**Figure 2** Ultrasound image of masseter registered using two parallel scan sweeps. A more complete image has been produced than would have been possible using only a single sweep.

capture as much of the muscle width as possible (Figure 1), later images were produced using multiple parallel scan sweeps (Figure 2). In these cases, the first sweep was carried out as for a single sweep scan, following which the computer software enabled parallel displacements of the sweep to fill in any missed portions of the anterior and posterior muscle borders.

Three-dimensional data acquisition was by means of a specially developed system (Gardener, 1991), based on a video frame grabber (The Harlequin™, Quintek Ltd, Westbury-on-Trym, Bristol, UK) linked to a computer, which allowed video images to be stored at the update rates of most US scanners. The scans were recorded as

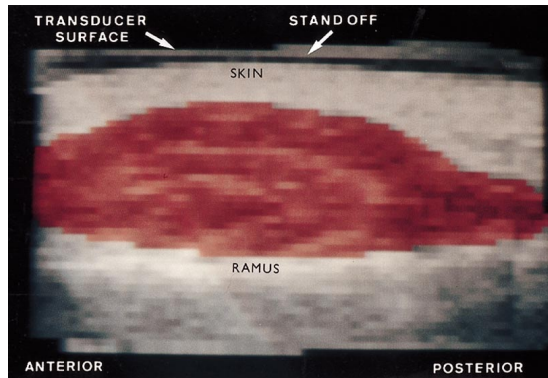


**Figure 3** Masseter scan on which the muscle boundary has been delineated using a cursor. This enabled the area composed of muscle to be identified by the computer. An estimated boundary has been inserted where the muscle image is incomplete at its anterior border.

a series of slices using positional information from a magnetic 3D sensor attached to the US probe. This enabled each component of the signal to be assigned its correct position in 3D image space. The images were reconstructed by the computer into an array of typically,  $128 \times 128 \times 100$  voxels and displayed as a series of consecutive 'slices' at intervals of 1.56 mm on a 3D workstation (Linney *et al.*, 1989).

To enable the computer to identify the image area composed of muscle, thresholding was employed to adjust the ultrasonic signal level in order to achieve optimal visualization of those elements of the image to be judged as masseter. The boundaries of masseter were then manually outlined on alternate slices using a cursor (Figure 3). Where sections of the images were missing or poorly defined, an estimated boundary was inserted. The interval between outlined images was thus 3.12 mm. When reconstructing the complete muscle image the computer interpolated the muscle contour in between slices. Each slice, therefore, represented a volume of muscle equal to its cross-sectional area multiplied by the slice interval. The complete array of delineated slices representing the 3D muscle image was then displayed, and could be rotated and viewed in all three planes of space, as could selected individual slices or sections of the image.

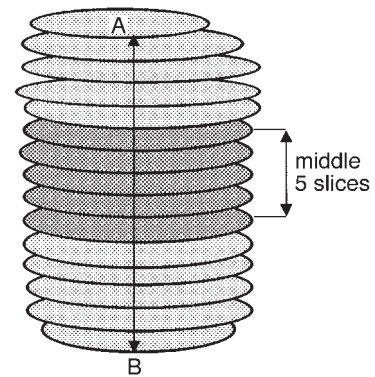


**Figure 4** Diagrammatic representation of masseter image consisting of an array of delineated muscle 'slices'. Volume measurement was computed from the total number of voxels occupied by the muscle image. Muscle length was measured by the computer between cursors A and B, placed at the top and bottom of the image, in line with its long axis. The five darkly-shaded slices in the middle of the array represent those from which cross-sectional area, thickness, and width were calculated.

#### *Muscle measurements*

Volume measurement was based on a count of the number of 3D image volume elements (voxels) selected to represent the muscle, rather than using approximate geometric methods. This selection, or segmentation, was based upon the manual outlining process described above, which resulted in a proportion of the voxels being labelled as comprising the muscle volume. The voxel count was effected automatically by the computer software and allowed volume measurement to within an accuracy of  $1 \text{ mm}^3$ . Muscle length was computed by positioning a cursor at the top and bottom of the array of slices on the visual display unit (VDU), parallel with the long axis of the muscle image (Figure 4). The remaining measurements were made from the mid-belly portion of the muscle images (Figure 4), since this was found to be the most clearly defined. To calculate the mean mid-belly cross-sectional area, the volume of a five-slice section of the muscle image, equidistant from either end of the complete image, was divided by five times the slice thickness. To measure the mean mid-belly thickness (medio-laterally) and width (antero-posteriorly), three alternate slices from



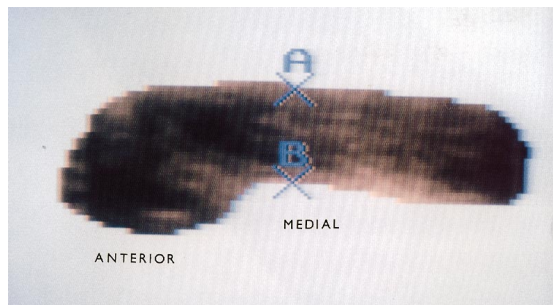


**Figure 5** Three alternate slices from the middle five-slice section of each muscle image were measured individually. Muscle thickness was recorded as the mean distance between points A and B at the antero-posterior midpoint of the muscle cross-section. Similarly, muscle width was measured by placing cursors at opposite ends of the same cross-sections.

the middle five-slice section were viewed individually in cross-section and measured using the VDU cursors (Figure 5).

### Cephalometry

Standardized lateral skull radiographs were taken for all subjects with the Frankfort plane horizontal and the teeth in occlusion. The landmarks were digitized and a cephalometric analysis carried out by the computer consisting of seven angular, eight linear and two proportional variables (Figures 6 and 7). The variables were selected so that the different dimensions of the facial skeleton were described by groups of inter-related angular and linear measurements, which were then reduced to four principal components by means of a principal component analysis.

### Sources of error

The US system was subject to errors inherent in the scanning technique, the image reconstruction process and the image measurement method. The orientation of the probe was maintained manually during scan registration. Kiliaridis and Kalebo (1991) stressed the importance of achieving scan planes perpendicular to the ramus of the mandible to minimize the possibility of erroneously large muscle thickness measurements. Cross-sectional area and width measurements

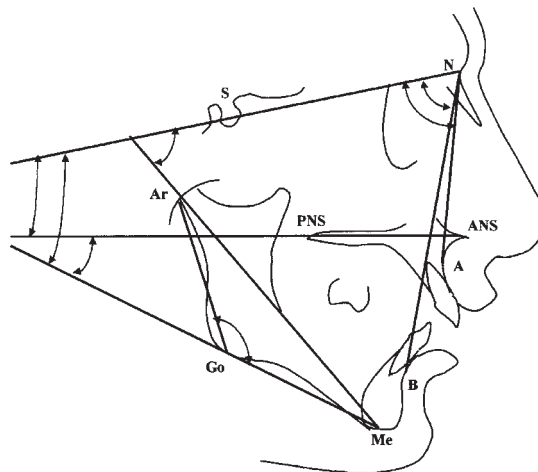


**Figure 6** Angular variables used in the principal component analysis: SNA, SNB, SN-Max, SN-Mand, Max-Mand, SN-Ar-Me, Ar-Go-Me. Max = maxillary plane (ANS-PNS); Mand = mandibular plane (Me-Go).

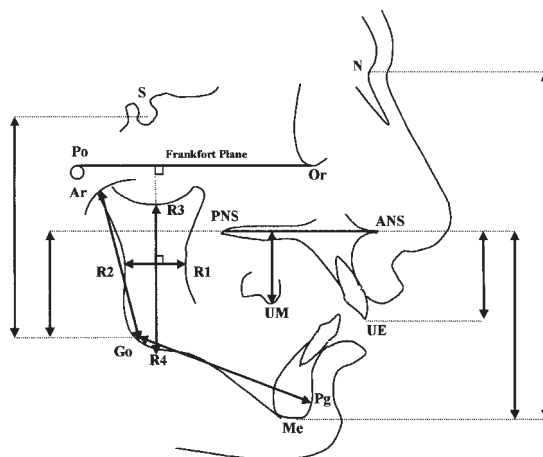


**Figure 7** Linear variables used in the principal component analysis: Ar-Go, Go-Pg, R1-R2, R3-R4, TAFH (the sum of SN-Max and Max-Me, perpendicular to Max), TPFH (the sum of S-Max and Max-Go, perpendicular to Max), UADH (UE-Max, perpendicular to Max), UPDH (UM-Max, perpendicular to Max). Proportional variables: LAFH/TAFH, LPFH/TPFH. Points R1-R4 are taken from Ricketts *et al.* (1972).

would also be affected in this study by angular deviations in probe position.

On the majority of scans, most of the width of the muscle was contained within the single swept

**Table 1** Error of the method.

| Masseter variable                      | Dahlberg error ( $S_e$ ) | Coefficient of reliability |
|--|--------------------------|----------------------------|
| Volume ( $\text{cm}^3$ )               | 0.93                     | 0.92                       |
| Cross-sectional area ( $\text{cm}^2$ ) | 0.21                     | 0.96                       |
| Thickness (mm)                         | 1.96                     | 0.50                       |
| Width (mm)                             | 2.03                     | 0.82                       |
| Length (mm)                            | 0.99                     | 0.98                       |

volume, but in some cases the muscle boundaries lay outside the transducer field, and boundary definition was frequently poor, even within the field of view. This latter problem is common with US and was due to poor reflection of US from edges parallel to the muscle boundary. To determine the error in muscle measurement, eight muscle image reconstructions were repeated a minimum of 1 week later, and the standard Dahlberg error (Dahlberg, 1940) and coefficient of reliability (Houston, 1983) calculated (Table 1).

**Table 3** Eigenvalues of the correlation matrix of the principal component analysis.

|       | Eigenvalue | Difference | Proportion | Cumulative |
|-------|------------|------------|------------|------------|
| PRIN1 | 12.1       | 4.9        | 0.41       | 0.41       |
| PRIN2 | 7.2        | 2.6        | 0.24       | 0.65       |
| PRIN3 | 4.6        | 2.1        | 0.15       | 0.80       |
| PRIN4 | 2.5        | 1.2        | 0.08       | 0.88       |
| PRIN5 | 1.3        | 0.4        | 0.05       | 0.93       |
| PRIN6 | 0.9        | 0.3        | 0.03       | 0.96       |
| PRIN7 | 0.6        | 0.2        | 0.02       | 0.98       |
| PRIN8 | 0.4        | 0.2        | 0.01       | 0.99       |
| PRIN9 | 0.2        | 0.1        | 0.01       | 1.00       |

## Results

The results of the cephalometric analysis are shown in Table 2, and the eigenvalues of the correlation matrix of the principal component analysis in Table 3. The principal components are arranged in descending order of variance, the first nine accounting for the total variance in the original data. As the first four accounted for most of the variance (88 per cent) with the

**Table 2** Values and descriptive statistics for cephalometric variables used in the principal component analysis.

| Variables    | Male subjects |       |       |       | Female subjects |       |       |       |       |       | Descriptive statistics |       |       |      |
|--------------|---------------|-------|-------|-------|-----------------|-------|-------|-------|-------|-------|------------------------|-------|-------|------|
|              | 1             | 2     | 3     | 4     | 5               | 6     | 7     | 8     | 9     | 10    | Min.                   | Max.  | Mean  | SD   |
| Angular      |               |       |       |       |                 |       |       |       |       |       |                        |       |       |      |
| SNA          | 82.7          | 83.5  | 85.2  | 83.0  | 73.7            | 83.3  | 78.5  | 78.2  | 83.0  | 80.5  | 73.7                   | 85.2  | 81.2  | 3.5  |
| SNB          | 80.8          | 86.8  | 81.2  | 77.2  | 73.5            | 81.8  | 82.8  | 73.2  | 73.0  | 69.7  | 69.7                   | 86.8  | 78.0  | 5.5  |
| SN-Mand.     | 41.5          | 30.2  | 17.3  | 32.0  | 41.7            | 36.3  | 33.8  | 48.5  | 45.7  | 52.0  | 17.3                   | 52.0  | 37.9  | 10.2 |
| SN-Max.      | 13.2          | 4.3   | 6.2   | 9.0   | 8.0             | 8.7   | 4.0   | 4.3   | 7.2   | 8.3   | 4.0                    | 13.2  | 7.3   | 2.8  |
| Max-Mand     | 28.2          | 26.0  | 11.2  | 23.0  | 33.8            | 27.7  | 30.0  | 44.2  | 38.5  | 43.8  | 11.2                   | 44.2  | 30.6  | 10.0 |
| SN-Ar-Me     | 58.0          | 52.7  | 39.7  | 54.7  | 58.3            | 53.5  | 54.0  | 66.0  | 64.3  | 66.7  | 39.7                   | 66.7  | 56.8  | 8.0  |
| Ar-Go-Me     | 140.2         | 124.0 | 124.5 | 123.2 | 132.7           | 134.5 | 126.0 | 131.5 | 135.2 | 142.5 | 123.2                  | 142.5 | 131.4 | 6.9  |
| Linear       |               |       |       |       |                 |       |       |       |       |       |                        |       |       |      |
| Ar-Go        | 50.5          | 51.7  | 49.2  | 47.8  | 39.7            | 43.8  | 46.7  | 37.0  | 43.2  | 38.0  | 37.0                   | 51.7  | 44.8  | 5.3  |
| Go-Pg        | 74.0          | 78.8  | 75.8  | 74.8  | 72.3            | 71.2  | 76.0  | 64.3  | 59.7  | 59.8  | 59.7                   | 78.8  | 70.7  | 6.9  |
| R1-R2        | 26.5          | 32.7  | 33.0  | 33.0  | 21.7            | 26.3  | 31.3  | 27.8  | 26.0  | 22.7  | 21.7                   | 33.0  | 28.1  | 4.2  |
| R3-R4        | 55.3          | 55.0  | 44.2  | 56.3  | 41.7            | 43.3  | 55.0  | 48.3  | 44.8  | 43.5  | 41.7                   | 56.3  | 48.7  | 5.9  |
| TAFH         | 137.3         | 119.0 | 105.3 | 124.0 | 111.7           | 112.3 | 115.8 | 118.2 | 110.3 | 115.7 | 105.3                  | 137.3 | 117.0 | 8.8  |
| TPFH         | 87.2          | 81.5  | 84.0  | 84.3  | 62.8            | 70.5  | 74.8  | 69.0  | 65.2  | 64.7  | 62.8                   | 87.2  | 74.4  | 9.2  |
| UPDH         | 28.2          | 24.2  | 19.5  | 23.7  | 23.0            | 21.0  | 26.0  | 26.2  | 23.0  | 26.5  | 19.5                   | 28.2  | 24.1  | 2.7  |
| UADH         | 30.0          | 29.0  | 20.5  | 28.8  | 26.7            | 26.0  | 28.7  | 30.2  | 28.3  | 31.5  | 20.5                   | 31.5  | 28.0  | 18.6 |
| Proportional |               |       |       |       |                 |       |       |       |       |       |                        |       |       |      |
| LAFH/TAFH    | 58.0          | 57.7  | 50.7  | 55.0  | 59.0            | 56.7  | 61.3  | 58.3  | 58.7  | 55.3  | 50.7                   | 61.3  | 57.1  | 2.9  |
| LPFH/TPFH    | 53.0          | 44.0  | 46.7  | 49.0  | 42.3            | 44.3  | 45.3  | 36.0  | 42.0  | 35.3  | 35.3                   | 53.0  | 43.8  | 5.4  |

**Table 4** Eigenvector coefficients of cephalometric variables for the first four principal components.

| Angular variable | PRIN1 | PRIN2 | PRIN3 | PRIN4 | Linear variable | PRIN1 | PRIN2 | PRIN3 | PRIN4 |
|------------------|-------|-------|-------|-------|-----------------|-------|-------|-------|-------|
| SNA              | 0.17  | 0.07  | 0.22  | 0.12  | Ar-Go           | 0.31  | 0.11  | -0.03 | 0.10  |
| SNB              | 0.24  | -0.06 | -0.39 | -0.02 | Go-Pg           | 0.21  | 0.10  | -0.24 | -0.01 |
| SN-Mand          | -0.35 | 0.19  | -0.07 | 0.00  | R1-R2           | 0.23  | 0.27  | -0.13 | -0.24 |
| SN-Max           | -0.03 | 0.21  | 0.06  | 0.50  | R3-R4           | 0.15  | 0.09  | 0.11  | -0.31 |
| Max-Mand         | -0.30 | 0.09  | -0.09 | -0.14 | TAFH            | 0.05  | 0.35  | -0.09 | 0.03  |
| SN-Ar-Me         | -0.25 | 0.19  | -0.07 | -0.09 | TPFH            | 0.31  | 0.15  | 0.11  | -0.01 |
| Ar-Go-Me         | -0.24 | 0.16  | -0.01 | 0.29  | UPDH            | -0.11 | 0.30  | -0.15 | -0.14 |
|                  |       |       |       |       | UADH            | 0.10  | 0.05  | -0.09 | 0.44  |

**Table 5** Descriptive statistics for masseter muscle variables.

| Masseter variable                       | Min. | Max. | Mean | SD  |
|---|------|------|------|-----|
| <b>Males</b>                            |      |      |      |     |
| Volume (cm <sup>3</sup> )               | 16.1 | 32.7 | 23.0 | 7.1 |
| Cross-sectional area (cm <sup>2</sup> ) | 3.6  | 5.7  | 4.6  | 9.8 |
| Thickness (mm)                          | 9.6  | 13.1 | 11.1 | 1.3 |
| Width (mm)                              | 36.0 | 45.3 | 40.8 | 4.3 |
| Length (mm)                             | 45.9 | 62.0 | 53.8 | 5.8 |
| <b>Females</b>                          |      |      |      |     |
| Volume (cm <sup>3</sup> )               | 10.4 | 12.6 | 11.3 | 0.8 |
| Cross-sectional area (cm <sup>2</sup> ) | 2.2  | 3.5  | 3.1  | 0.4 |
| Thickness (mm)                          | 7.3  | 10.9 | 9.5  | 1.2 |
| Width (mm)                              | 26.8 | 38.8 | 34.2 | 4.1 |
| Length (mm)                             | 39.1 | 62.2 | 46.5 | 8.2 |

remainder adding little more than 10 per cent to the cumulative total, comparative statistical analysis was limited to the first four principal components.

The eigenvectors of the first four principal components are given in Table 4. The variance of the first principal component was largely accounted for by the negatively weighted angular measurements SN-Mand and Max-Mand (mandibular inclination) and the positively weighted linear measurements Ar-Go (ramus height) and total posterior face height (TPFH). Smaller contributions were provided by negatively loaded angles SN-Ar-Me and Ar-Go-Me (gonial angle).

The variance of the second component showed a large positively weighted contribution from the total anterior face height (TAFH), the maxillary posterior dentoalveolar height (UPDH) and

the width of the mandibular ramus (R1-R2). The third component showed a large negative loading for the angle SNB and the mandibular body length (Go-Pg). By far the largest weighting for the fourth component was from the inclination of the maxilla to the cranial base (SN-Max), with a lesser contribution from the positively weighted gonial angle and the negatively weighted ramus height.

The masseter muscle measurements for males and females are recorded in Table 5. To determine whether or not a correlation existed between facial morphology and masseter size, Spearman's rank correlation coefficients were calculated between the first four principal components of the cephalometric variables and each of the muscle variables, and between the proportional cephalometric variables and the muscle variables (Table 6). To test for any significant differences between the muscle volumes or cross-sectional areas in males and females, Wilcoxon's two-sample rank sum test was used. However, this proved non-significant for both of these variables.

## Discussion

Several investigators have attempted to measure masseter muscle size using imaging techniques. US has been used to measure thickness (Kiliaridis and Kalebo, 1991; Bakke *et al.*, 1992; Raadsheer *et al.*, 1994; Ruf *et al.*, 1994; Kubota *et al.*, 1998), width (Ruf *et al.*, 1994) and cross-sectional area (Ruf *et al.*, 1994; Close *et al.*, 1995). Cross-sectional area has also been measured

**Table 6** Spearman's rank correlation coefficient (*r*).

## (A) Principal components and muscular variables.

|   | PRIN1   | PRIN2 | PRIN3 | PRIN4 |
|---|---------|-------|-------|-------|
| Volume (cm <sup>2</sup> )               | 0.92*** | 0.11  | -0.10 | -0.20 |
| Cross-sectional area (cm <sup>2</sup> ) | 0.62    | 0.33  | 0.28  | -0.13 |
| Thickness (mm)                          | 0.39    | 0.40  | 0.19  | 0.05  |
| Width (mm)                              | 0.51    | 0.09  | -0.08 | -0.52 |
| Length (mm)                             | 0.76*   | 0.18  | 0.29  | -0.18 |

\**P* ≤ 0.05; \*\*\**P* ≤ 0.001.

## (B) Proportional cephalometric and muscular variables.

|   | LAFH/TAFH | LPFH/TPFH |
|---|-----------|-----------|
| Volume (cm <sup>2</sup> )               | -0.38     | 0.77**    |
| Cross-sectional area (cm <sup>2</sup> ) | -0.53     | 0.48      |
| Thickness (mm)                          | -0.63*    | 0.33      |
| Width (mm)                              | -0.04     | 0.26      |
| Length (mm)                             | -0.47     | 0.54      |

\**P* ≤ 0.05; \*\**P* ≤ 0.01.

using MRI (Hannam and Wood, 1989; van Spronsen *et al.*, 1991; Raadsheer *et al.*, 1994) and CT (Weijs and Hillen, 1984a, 1986; Gionhaku and Lowe, 1989; Xu *et al.*, 1994). Volume was measured using CT by Gionhaku and Lowe (1989), Xu *et al.* (1994) and Matsushima *et al.* (1998). No report has been published to date of masseter volume measurement using US.

### Ultrasonography

The scanning, reconstruction and display techniques used in this study represent only the first stage of 3D US capabilities. New techniques are currently being developed that will particularly benefit facial studies. These include improved scan 'registration' and 'compounding' to visualize the muscle structures more clearly, thus minimizing the distortion artefacts common to all US techniques. This, in turn, will allow development of better 'segmentation' methods for mathematically delineating the muscle boundaries. In addition, state-of-the-art hardware will allow more rapid scan collection in greater volumes.

'Compounding' refers to scanning tissues from more than one angle, thereby minimizing well-known US effects such as 'drop-out', which can cause indistinct rendering of organ boundaries. 'Registration' refers to the process whereby the images produced by multiple passes over the tissue from different directions are brought into accurate alignment. Several effects can cause misalignment, including scanner precision, tissue movement, and differences of sound velocities. Precise registration is essential in compounded scanning. 'Segmentation' refers to the process of defining the boundaries of images of organs. The muscle tissue may be segmented independently in cross-section and length. Automated or semi-automated methods could provide more reliable estimates of organ dimensions in the future, although the development of US segmentation is still at an early stage.

The system used in this study requires further evaluation to test its accuracy at data acquisition. An error study of repeated muscle scans would help to clarify this, as well as a calibration test using 'phantom' muscles of known volumes, similar to the method used by Xu *et al.* (1994). A comparison of US muscle volume measurements with those derived from CT or MRI scans of the same subjects would be valuable.

### Subjects and methods

The experimental nature of the 3D US system used in this study made scan registration, image reconstruction, and measurements time consuming, thus limiting the sample size. Subjects with severe malocclusions were selected because correlations are more likely to be revealed between facial morphology and masseter size if there is a large variance in the data.

In this study only clenched muscle scans were registered, since image boundary definition for muscles in the relaxed state was found to be inadequate to allow accurate segmentation. In addition, it was found by Raadsheer *et al.* (1994) and Kiliaridis and Kalebo (1991) that the transducer tends to compress relaxed muscles, resulting in erroneously small thickness measurements and making them less reproducible than clenched scans. The evidence as to whether contracted or



relaxed muscles correlate more closely with facial form is conflicting. Weijs and Hillen (1984a), van Spronsen *et al.* (1991), and Kiliaridis and Kalebo (1991) showed significance with measurements from relaxed muscle images, while Weijs and Hillen (1986), Hannam and Wood (1989), and Gionhaku and Lowe (1989) did not specify the muscle state during scanning. Bakke *et al.* (1992) stressed the importance of clenched muscle measurements, finding correlations with certain cephalometric variables, and Kubota *et al.* (1998) found significant correlations with masseter thickness in both the relaxed and clenched states.

## Results

Table 7 lists the measurement values recorded in this study along with those of previous investigators. The mean masseter muscle volume for males was  $23.0 \pm 7.1 \text{ cm}^3$ . This is less than the value of Gionhaku and Lowe (1989), but in closer agreement with that of Xu *et al.* (1994). Matsushima *et al.* (1998) measured the volume of masseter muscle using CT in a mixed sex sample and recorded a mean value of  $34.9 \text{ cm}^3$ . The mean volume for females was  $11.3 \pm 0.7 \text{ cm}^3$ , which is considerably less than that found by Xu *et al.* (1994). This might be due to the high proportion of long facial types among the females scanned in this study (see Table 2). Previous work has suggested that masseter size was reduced in subjects with long faces. Although Xu *et al.* (1994) did not carry out a cephalometric analysis of their subjects, their larger sample size (25 females) may have possessed a more normal distribution of facial variance, reflected in a more normal mean masseter volume.

The mean cross-sectional area value for males of  $4.6 \pm 1.0 \text{ cm}^2$  found in this study is broadly consistent with that of previous investigators (Hannam and Wood, 1989, and van Spronsen *et al.*, 1991, using MRI; Weijs and Hillen, 1984b, and Xu *et al.*, 1994, using CT; Close *et al.*, 1995, using US). Gionhaku and Lowe (1989) recorded a considerably larger figure for males using CT, but as they reported, the scan planes in their study were registered parallel to the Frankfort plane and this may have resulted in larger measurements.

The mean muscle thickness values were  $11.1 \pm 1.3 \text{ mm}$  for males and  $9.5 \pm 1.2 \text{ mm}$  for females in this study. These are less than those found by Kiliaridis and Kalebo (1991), Bakke *et al.* (1992), Raadsheer *et al.* (1994), Ruf *et al.* (1994), and Kubota *et al.* (1998). This may be because, in this investigation, thickness was measured at the antero-posterior midpoint of the muscle belly. Previous investigators have measured at the point of estimated maximum thickness (Kiliaridis and Kalebo, 1991; Raadsheer *et al.*, 1994; Ruf *et al.*, 1994) or recorded the mean of several measurements along the width of the muscle belly (Kubota *et al.*, 1998). Although Bakke *et al.* (1992) also measured thickness at the antero-posterior midpoint, their measurements were taken at the level where the muscle was estimated to be most bulky. In this study, three alternate slices from the middle of the muscle belly were selected, since this region was found to be the most clearly defined and, therefore, the most accurately measurable.

The mean values found in this study for muscle width were  $40.8 \pm 4.3 \text{ mm}$  for males and  $34.2 \pm 4.1 \text{ mm}$  for females. Ruf *et al.* (1994) used US to measure masseter width parallel to the occlusal plane and recorded larger figures than these, but their measurements may have been taken from oblique scan planes, since Hannam and Wood (1989) found that the functional occlusal plane was not perpendicular to the long axis of masseter muscle. Ultrasound image measurements are also prone to systematic errors at the boundary definition stage due to the phenomenon of 'point spreading', where a relatively thick line on the image display represents what is actually a sharp tissue boundary. In this study, the muscle boundary was demarcated for measurement purposes completely within the image boundary line. Some other investigators may have partly or completely included the image boundary line in their measurements, resulting in comparatively larger values.

Male muscle measurements tended to be larger than female muscle measurements. The lack of significance of Wilcoxon's rank sum coefficient for cross-sectional area and volume is probably best explained by the small sample size. This observed difference may be partly the result of natural sexual dimorphism, but has probably



been accentuated by the difference in facial morphology between the sexes in this study. The males had a tendency to short face features, while the females had long face characteristics. Kiliaridis and Kalebo (1991), in a sample of 20 males and 20 females, found significantly larger values for masseter thickness in males.

Spearman's rank correlation coefficient was used to relate each of the five muscle variables to the four principal components of facial form and the two proportional variables (LAFH/TAFH, LPFH/TPFH). The first principal component showed a significant, positive correlation with masseter muscle volume ( $r = 0.92$ ,  $P \leq 0.001$ ) and muscle length ( $r = 0.76$ ,  $P \leq 0.05$ ), while LPFH/TPFH correlated significantly and positively with volume ( $r = 0.77$ ,  $P \leq 0.01$ ). This indicates a negative correlation of masseter muscle volume and length with mandibular inclination, including gonial angle, and a positive correlation with mandibular ramus height and total posterior face height. These findings are consistent with those of previous investigators. Gionhaku and Lowe (1989) found negative correlations for masseter muscle volume with mandibular plane and gonial angles, and a positive correlation with posterior face height and ramus height, while Eckhardt and Harzer (1993) found that 'increasing volume of masseter correlated with an anterior growth direction'.

LAFH/TAFH correlated negatively with muscle thickness ( $r = -0.63$ ,  $P \leq 0.05$ ). Thin masseters were associated, therefore, with subjects possessing long faces. Kiliaridis and Kalebo (1991) found that women with thin masseters had proportionately longer faces, while Bakke *et al.* (1992) found negative correlations above the 95 per cent confidence level between the contracted thickness of masseter and the height of the face and jaws, mandibular inclination and vertical jaw relationship.

The correlation of muscle length with the first principal component found in this study reflects the tendency for short-faced subjects to possess large posterior face heights (Opdebeeck and Bell, 1978). No significant correlations were found for muscle width or cross-sectional area with any of the facial variables, but this may be a reflection of the small sample size.

## Conclusions

The following conclusions were drawn from the study.

1. The specialized computer software used for US image reconstruction enabled 3D measurements to be made of masseter muscle including volume. However, comparison with other accepted standards, namely CT and MRI, as well as further calibration, is necessary to establish the effectiveness of the system.
2. Discrepancies between the muscle measurement values in this study and those found by other investigators may be due to disparities between the samples, differences in the location of muscle measurement points, and the use of different imaging techniques by different investigators.
3. In the subjects studied, statistical analysis showed that a steeply inclined mandibular plane, a small posterior face height, and an increased gonial angle were strongly related to short, thin masseter muscles of low volume. Long, thick muscles of high volume were related to the converse features. These results must be interpreted with caution in view of the small sample size.
4. The 3D US system was acceptable to patients and relatively straightforward to use, but requires further development to overcome some of the problems inherent in acoustic imaging, in particular organ boundary definition.

## Address for correspondence

Professor N. P. Hunt  
Orthodontic Department  
Eastman Dental Institute  
256 Gray's Inn Road  
London WC1X 8LD, UK

## Acknowledgements

We wish to express our sincere thanks to Professor W. R. Lees, for permitting use of the ultrasound scanner at the Middlesex Hospital, London, and to Dr J. Bulman, for help with the statistics. Mr A. J. Hart kindly wrote the cephalometric digitization program.

## References

- Ahlgren J 1966 Mechanism of mastication. A quantitative cinematographic and electromyographic study of masticatory movements in children, with special reference to occlusion of the teeth. *Acta Odontologica Scandinavica* 24 (Suppl. 44): 1–109
- Bakke M, Tuxen A, Vilmann P, Jensen B R, Vilmann A, Toft M 1992 Ultrasound image of human masseter muscle related to bite force, electromyography, facial morphology, and occlusal factors. *Scandinavian Journal of Dental Research* 100: 165–171
- Close P J, Stokes M J, L'Estrange P R, Rowell J 1995 Ultrasonography of masseter muscle size in normal young adults. *Journal of Oral Rehabilitation* 22: 129–134
- Dahlberg G 1940 Statistical methods for medical and biological students. Interscience Publications, New York
- Eckardt L, Harzer W 1993 Computertomographic volume registration of jaw and tongue muscles in consideration of relationship between function of muscles and skeletal configuration. *European Journal of Orthodontics* 15: 442 (Abstract)
- Gardener J E 1991 Three-dimensional imaging of soft tissues using ultrasound. 3D Imaging for Medicine. IEE Colloquium digest 91/083: Institute of Electrical Engineers, London
- Gionhaku N, Lowe A A 1989 Relationship between jaw muscle volume and craniofacial form. *Journal of Dental Research* 68: 805–809
- Hannam A G, Wood W W 1989 Relationships between the size and spatial morphology of human masseter and medial pterygoid muscles, the craniofacial skeleton, and jaw biomechanics. *American Journal of Physical Anthropology* 80: 429–445
- Hell B 1995 3D Sonography. *International Journal of Oral and Maxillofacial Surgery* 24: 84–89
- Hell B, Walter F A, Schreiber St., Blase H, Bielke G, Meindl St., Stein G 1993 Three-dimensional ultrasonography in maxillofacial surgery. *International Journal of Oral and Maxillofacial Surgery* 22: 173–177
- Houston W J B 1983 The analysis of errors in orthodontic measurements. *American Journal Orthodontics* 83: 382–390
- Ingervall B, Helkimo E 1978 Masticatory muscle force and facial morphology. *Archives of Oral Biology* 23: 203–206
- Ingervall B, Thilander B 1974 Relation between facial morphology and activity of the masticatory muscles. *Journal of Oral Rehabilitation* 1: 131–147
- Kiliaridis S, Kalebo P 1991 Masseter muscle thickness measured by ultrasonography and its relation to facial morphology. *Journal of Dental Research* 70: 1262–1265
- Kubota M, Nakano H, Sanjo I, Satoh K, Sanjo T, Kamegai T, Ishikawa F 1998 Maxillofacial morphology and masseter muscle thickness in adults. *European Journal of Orthodontics* 20: 535–542
- Linney A D, Grindrod S R, Arridge S R, Moss J P 1989 Three-dimensional visualisation of computerised tomography and laser scan data for the simulation of maxillo-facial surgery. *Medical Informatics* 14: 109–121
- Lowe A A, Takada K 1984 Association between anterior temporal, masseter, and orbicularis oris muscle activity and craniofacial morphology in children. *American Journal of Orthodontics* 86: 319–330
- Matsushima S, *et al.* 1998 Relationship between the volume of masticatory muscles and dentofacial morphology. *European Journal of Orthodontics* 20: 475–476
- Opdebeek H, Bell W H 1978 The short face syndrome. *American Journal of Orthodontics* 73: 499–511
- Proffit W R, Fields H W, Nixon W L 1983 Occlusal forces in normal- and long-face adults. *Journal of Dental Research* 62: 566–571
- Raadsheer M C, Eijden T M G J, van Spronsen P H, van Ginkel F C, Kiliaridis S, Prah-Andersen B 1994 A comparison of human masseter muscle thickness measured by ultrasonography and magnetic resonance imaging. *Archives of Oral Biology* 39: 1079–1084
- Ricketts R, Bench R W, Hilgeis J J, Schulhof R 1972 An overview of computerised cephalometrics. *American Journal of Orthodontics* 61: 1–28
- Ringqvist M 1973 Isometric bite force and its relation to dimensions of the facial skeleton. *Acta Odontologica Scandinavica* 31: 35–42
- Ruf S, Pancherz H, Kirschbaum M 1994 Gesichtsmorphologie, Grosse und Aktivität des Musculus masseter. *Fortschritte der Kieferorthopädie* 23: 219–227
- Sassouni V 1969 A classification of skeletal facial types. *American Journal of Orthodontics* 55: 109–123
- Schendel S A, Eisenfeld J, Bell W H, Epker B N, Mishelevich D J 1976 The long face syndrome: vertical maxillary excess. *American Journal of Orthodontics* 70: 398–408
- Ueda H M, Ishizuka Y, Miyamoto K, Morimoto N, Tanne K 1998 Relationship between masticatory muscle activity and vertical craniofacial morphology. *Angle Orthodontist* 68: 233–238
- van Spronsen, P H, Weijs W A, Valk J, Prah-Andersen B, van Ginkel F C 1991 Relationships between jaw muscle cross-sections and craniofacial morphology in normal adults, studied with magnetic resonance imaging. *European Journal of Orthodontics* 13: 351–361
- Weijs W A, Hillen B 1984a Relationships between masticatory muscle cross-section and skull shape. *Journal of Dental Research* 63: 1154–1157
- Weijs W A, Hillen B 1984b The relationship between the physiological cross-section of the human jaw muscles and their cross-sectional area in computer tomograms. *Acta Anatomica* 118: 129–138
- Weijs W A, Hillen B 1986 Correlation between the cross-sectional area of the jaw muscles and craniofacial size and shape. *American Journal of Physical Anthropology* 70: 423–431
- Xu J A, Yuasa K, Kanda S 1994 Quantitative analysis of masticatory muscles using computed tomography. *Dento-maxillofacial Radiography* 23: 154–158